Geochemistry and tectonic setting of Maien Bolagh (Takab) alkali gabbros-NW Iran

Monir Modjarrad

Department of Geology, University of Urmia, Urmia, Iran.

* Corresponding Author: m.modjarrad@urmia.ac.ir

Received: 19 October 2013 / Accepted: 07 December 2013 / Published online: 10 December 2013

Abstract

Some small gabbro patches emplaced along the thrust fault with W-E trend in the vicinity of Maien Bolagh village at the HT/MP metapelites, a part of the Central Iran zone (near to Sanandaj-Sirjan zone). The coarse-grained dark gabbro samples consist of amphibole, clinopyroxene, plagioclase, minor quartz, titanite, and biotite. Gabbros have high potassic calc-alkaline to shoshonitic affinity. The highly incompatible elements concentrations (e.g. Nb and La) and Zr/Y and Zr/Nb ratios are similar to within plate gabbros. At the assorted discrimination diagrams the gabbros exhibit mostly non-orogenic resemblance. The geochemical characteristics show that the gabrros can be interpreted as melts formed from an enriched mantle in a passive rift position, during an extensional or transtensional tectonic.

Keywords: Gabbro; Maien Bolagh; Within Plate; Geochmistry.

1–Introduction

Alkaline magmatism is well represented in the continental areas with extensional tectonism (Wilson and Downes, 1991; Wedepohl *et al*., 1994; Wilson *et al*., 1995; Griffiths *et al*., 1997; Dostal and Owen, 1998; Ngounouno *et al*., 2001), though a gradual transition from orogenic calc-alkaline to continental intraplate alkaline magmatism has been documented in several regions (e.g. Stern *et al*., 1990; Coulon *et al*., 2002). In subduction-related regions, alkaline magmatism occurs in the back-arc domains and is generally related to an extentional regime that allows mantle upwelling and melt production by a slab rollback (Hole *et al*., 1995; Haschke *et al*., 2002).

The Sanandaj–Sirjan Zone (SSZ) is one of the most important tectonic sections of Iran that include numerous plutonic bodies. It is a part of the Zagros orogeny and divided into an outer belt of imbricate thrust slices that includes the Zagros suture and an inner belt of mainly Mesozoic metamorphic rocks (Mohajjel *et al*, 2003). Because of the SSZ is suture zone between Afro-Arabian and Iranian plates (Alavi, 2007), understanding its geological history could unravel the regional geology of adjacent areas (Ahadnezhad, 2013). The new zircon U-Pb crystallization ages unequivocally, demonstrate that crystalline basement underlying the Sanandaj–Sirjan zone ,central Iran, Alborz Mountains is composed of continental fragments with Gondwanian affiliation, characterized by wide spread late Neoproterozoic subduction-related magmatism (Hassanzadeh *et al*., 2008).

Different igneous and metamorphic rocks are exposed between Takab and Shahindezh area in the western Iran (Modjarrad, 2007) near the Sanandaj-Sirjan zone. On the basis of stratigraphic and field observations, metapelitic rocks are the oldest unit in this area. The metapelites have been subjected to two regional and one contact metamorphic events and at least three deformational phases (Modjarrad *et al*., 2008). Using major oxides elements, the continental active margin is considered for

metapelites source (Modjarrad *et al*., 2010). The leucogranite dykes and small S-type bodies intruded into them (Modjarrad, 2007). Upper Cretaceous marly limestones at the area (Fig. 1) are recrystallised as a result of Pichaghchi intrusion (at the south of the area) during Upper Cretaceous-Paleocene (Kholgi and Abedini, 2004). Maien Bolgh Gabbros (MBGs) are intruded at the metapelites along a fault with small exposure. Because of this size substance, the MBG is not reported at the Shahindezh 1:100000 sheet (Kholgi *et al*., 1994). In fact it is the first report of the unit at the Iran geological society. Hence there is no any dating on them, but the field evidences show that the MBG is younger than metapelites regional metamorphism at the upper cretaceous. Petrography, classification, geochemistry and general tectonic setting of the rocks are mentioned at this study.

2– Geological setting

Metamorphic rocks including metapelite, amphibolite, paragneiss and marble accompany the igneous rocks consisting of leucogranite, granodiorite and gabbro (Fig. 1). The Pan African orogeny which occurred at the Late Precambrian, caused faulting, folding and metamorphism of the Protrozoic and Archeozoic rocks at some parts of the Iranian crust (Darvish zadeh, 1990). The area is considered as Precambrian basement of Iran (Central Iran zone, Fig. 1, near to Sanandaj-Sirjan zone), which is deformed in during the Pan African orogeny (Berberian and King, 1981). On the basis of mineralogy, geochemistry and field relations, leucogranites resemble the first group of Precambrian magmatic rocks of Iran, (Aghanabati, 2006). Dolomitic rocks of the Soltaniyeh formation are exposed at the NW and SW of the study area (Fig. 1). It consists of Chuaria Circularis-bearing grey- brown shale indicating Vendian age.

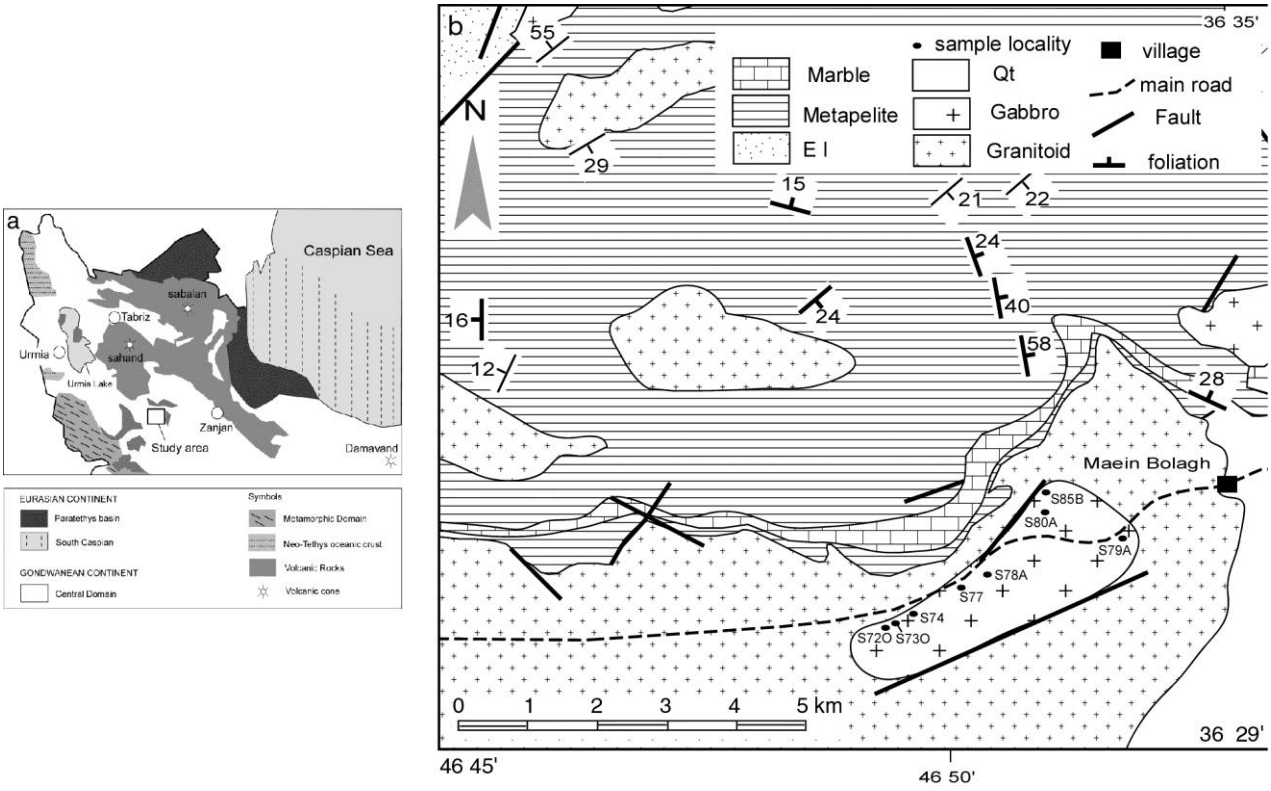

Figure 1 a) Structural zones of Iran after Aghanabati (2006) at the study area. b) Simplified geological map of the SMC, NW Iran, modified after (Modjarrad, 2007a). Sample locations are added.

Lalun formation sandstones are covered disconformably by the Upper Cambrian-Lower Ordovician Mila formation sediments (Kholgi *et al*., 1994). It seems that the area have been

uplifted after deposition of Mila formation during Middle and Upper Paleozoic (Kholgi *et al*., 1994, Fig. 1). The Pichaghchi granodiorite is an I-type granite with volcanic arc affinity (Modjarrad *et al*., 2007). Maien Bolagh gabbros (MBG) near the southeast part of Shahindezh to Takab road at the West Azarbaijan province of Iran have small exposure, near the Sanandaj-Sirjan zone. Coarse grain gabbros revealed along the thrust fault with W-E trend. The gabbros are not mentioned at the Geological Survey of Iran report (Kholgi *et al*., 1994), at the Shahindezh sheet. But some alkaline stocks are reported by Ghalamghash *et al* (2009) at the NW of Iran.

3– Petrography

The coarse-grained dark gabbro samples consist of amphibole, clinopyroxene, plagioclase, minor quartz, titanite, biotite and large idiomorph apatite, opaque and zircon, as accessory phases. Phenocrysts of amphibole (35 modal %) are subhedral to anhedral. The clinopyroxene phenocrysts (20 modal %) are subhedral to euhedral and pale green (apple green) which are occasionally altered to chlorite. The plagioclase crystals (30 modal %) are generally subhedral to anhedral laths and show often albite twinning. Euhedral titanite crystals are shown (probably as alteration product). Plagioclase and amphiboles are mostly fresh. Apatite is the most common accessory phase, occurring in large hexagonal crystals. All samples are olivine free. Equigranular and hypidiomorphic are the most common textures.

4– Analytical methods

Eight samples from the gabbros were analysed for whole-rock, major and trace elements and four representative samples from gabbros analysed for rare earth elements. These samples were analysed by a sequential X-ray flourescence spectrometer and inductively coupled plasma mass spectrometer at the ALS Chemex analytical laboratories Ltd., Canada and institute for geological sciences at the Potsdam University (GFZ), Germany.

5– Geochemistry

5.1– Major elements

All analyzed MBG samples (Table 1) are characterized by low SiO_2 contents (45.56-53.01 %) and medium to high values of MgO (7.35-11.46 %), TiO_2 (1.153-2.64 %), CaO (10.34-15.34 %), P_2O_5 (0.4-1.015), K_2O (0.81-1.70), Na_2O (1.74-3.37 %) and Al_2O_3 (9.0-13.72 %). A negative correlation is observed between SiO_2 and MgO, Fe_2O_3, CaO, TiO_2 and P_2O_5. A positive correlation is observed between SiO_2 content and Al_2O_3 and alkalies variations.

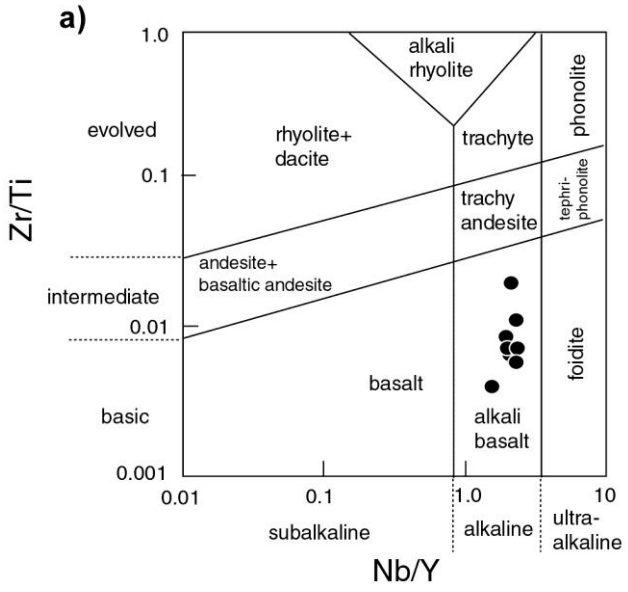

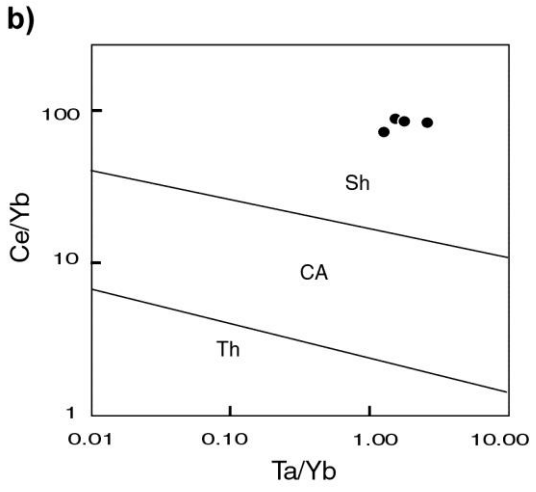

Figure 2a) Igneous rocks classifications after Middlemost (1995). All samples are alkali basalts. b) Shoshonitic affinity of MBG samples at the Muller and Groves (1993) diagram.

According to the total alkali content (ΣAlkali=2.58-4.74 %) the rocks plot on the boundary line between alkaline-subalkaline field (Irvine and Baragar, 1971) with a positive correlation between the SiO_2 content and the alkalies. Two samples have normative nephelin (1.37-1.46 %) and three samples have normative forstrite (Table 1). We used the total alkali vs. SiO_2 diagram of Middlemost (1991) for MBG nomenclature (Fig. 2a). MBG samples plot in the monzodiorite-gabbro-tonalite field. The MBG has high potassic calc-alkaline to shoshonitic affinity (Rickwood, 1989).

Relative to increasing SiO_2 abundance, the rocks show trends of decreasing MgO, Fe_2O_3 (t) and CaO indicates that crystal fractionation of mafic minerals was a significant processes in the genesis of the rocks, although crystal contamination can also result in the simultaneous increase of SiO_2 and incompatible elements and decrease of most compatible elements (e.g. MgO, Shinjo *et al*., 2000). The existence of negative correlation of MgO with Sr and Al_2O_3 indicates that plagioclase was not crystallized during the fractional crystallization processes and thus modally increased at the end of the process. The whole rock compositions are mostly Ti-and P-rich which is indicator of alkaline, within plate magmas. TiO_2 abundances decrease with increasing SiO_2, implying crystallization of titaniferous magnetite, suggesting relatively high fO_2 in the melt.

5.2– Trace elements

Incompatible trace elements (Zr, Nb, Y, Ba, Sr) are relatively enriched in the MBGs (Table 2). The magma was primitive mafic melts, in agreement with the high Ni (132-224 ppm, >150 for three samples) and Cr (100-970 ppm, >200 for three samples) concentrations (Wilson, 1993). The alkaline MBG, display the most primitive melts, as indicated by high Nb, MgO, Cr and Ni contents. The Ni, Cr, Co and V contents decrease with increasing the SiO2 content. It could be related to the fractional crystallization of pyroxene, amphibole and magnetite. The increasing trend of Rb, Ba, Sr and La with increasing the SiO_2 content, show that calcic plagioclase is not crystallize during early stages of cooling of magma. In order to identification of magmatic series by trace elements ratios we used the Moler and Groves (1993) graphs (Fig. 2b). All samples lie at the shoshonitic field.

5.2– Rare earth elements

The chondrite-normalized REE diagram (Fig. 3) shows a parallel pattern for all the MBG samples. The REE patterns of the MBG exhibit enrichment in LREE and depletion in HREE. The REE patterns do not show any Eu anomalies.

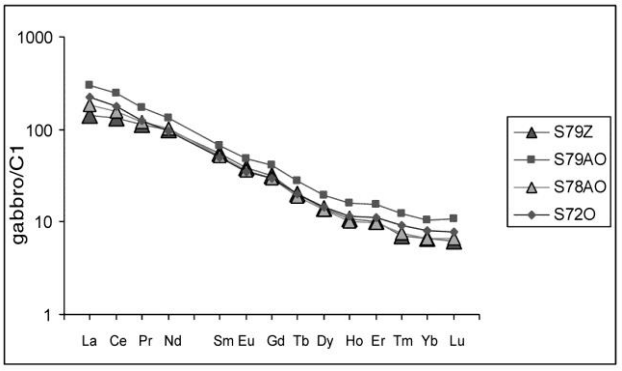

Figure 3) REE concentrations of MBG relative to C1chondorite values from (Sun and McDonough, 1989).

The MBG pattern exhibits a LREE enrichment of ~300 times chondritic and a negative slope with a La_N/Yb_N ratio of approximately 21-28. This characteristic is expressed on the emphatic negative slope. The observed high La_N/Yb_N reveal a low degree of mantle melting in the source region (Nakamura *et al*., 1989; Ramos and Kay, 1992) and a strongly LREE-enriched mantle source. The REE patterns of the MBG are similar to those of the alkaline OIB (Sun and McDonough, 1989). The Yb_N and Lu_N values

(<10) may indicate the presence of garnet as residual phase in the mantle source. $(La/Lu)_N$ ratios range from 21.51 to 27.5 and no Eu anomaly is observed (Fig. 3). An additional La enrichment is possible due to crystal fractionation (Haschke *et al*., 2002).

Table 1) Major element analyses and calculated normative mineral abundances of MBG, NW-Iran.

	S72O	S78A	S79A	S74	S77	S73O	S80A	S85B
SiO_2	53.01	47.43	48.63	45.56	52.8	47.3	48.3	53.0
Al_2O_3	11.63	9.33	13.72	9.12	11.2	9.0	13.5	11.1
Fe_2O_3	7.98	8.81	9.23	10.38	8.16	9.02	9.49	7.94
CaO	10.68	14.72	10.34	14.88	11.11	15.34	10.88	10.96
MgO	7.35	11.05	7.48	10.77	7.61	11.46	7.89	8.44
Na_2O	3.08	2.00	2.98	1.74	3.08	2.01	3.04	3.37
K_2O	1.38	0.98	1.66	0.84	1.38	0.98	1.70	0.81
TiO_2	1.78	1.93	2.64	2.41	1.604	1.816	2.530	1.153
MnO	0.13	0.12	0.11	0.13	0.134	0.125	0.119	0.161
P_2O_5	0.4	0.63	0.56	0.71	0.432	0.661	0.57	1.015
LOI	1.45	1.06	0.88	1.59	_	_	_	_
H_2O	_	_	_	_	1.26	1.10	0.97	1.29
CO_2	_	_	_	_	1.26	1.10	0.97	1.29
Total	98.96	98.35	98.47	98.4	99.4	99.2	99.3	99.6
Q	3.65	0.00	0.00	0.00	2.63	0	0	2.72
Or	8.39	5.98	10.09	5.15	8.37	5.93	10.26	4.9
Ab	26.75	14.90	25.87	12.54	26.7	11.6	24.47	29.11
An	14.18	13.98	19.64	15.09	12.96	12.91	18.5	12.75
Ne	0.00	1.37	0.00	1.46	0	3.14	0.95	0
Di wo	15.80	24.01	12.40	23.83	17.11	25.47	13.85	15.34
Di en	12.14	18.52	9.62	17.85	12.97	19.44	10.76	11.53
Di fs	1.96	2.87	1.40	3.55	2.35	3.32	1.55	2.24
Hy en	6.74	0.00	3.47	0.00	6.54	0	0	10.04
Hy fs	1.09	0.00	0.50	0.00	1.18	0	0	1.95
Ol fo	0.00	6.97	4.28	7.03	0	6.91	6.55	0
Ol fa	0.00	1.19	0.69	1.54	0	1.3	1.04	0
Mt	4.93	5.01	5.63	5.62	5.1	4.96	5.9	4.93
Ilm	3.47	3.78	5.15	4.74	3.13	3.53	4.9	2.24
Ap	0.90	1.42	1.26	1.61	0.97	1.48	1.27	2.26

6– Tectonic Setting

Although MBG samples give rather low LOI (0.88-1.59), hence we can use many of the standard major element plots, but the HFSE and REE which are relatively immobile during alteration have been used to deduce the tectonic setting of the MBG.

The low Th/La ratios (av: 0.13) are similar to those of the primitive mantle (0.12, Sun and McDonough, 1989), Ba/Nb (17.89), Ba/Th (120.23), Th/Yb (0.19), K/Nb (352), Th/La (0.13) and Ba/La (12.4) ratios are typical of an EM-type reservoir (Sun and McDonough, 1989). As we previously noted, Yb_N values<10 affirm the presence of garnet as a residual phase in the source.

In the various discrimination diagrams the MBG display mostly non-orogenic affinity (Figs. 4 and 5). On the basis of P_2O_5 vs. Zr and Zr/TiO_2 vs. Nb/Y and Ti/Y vs. Nb/Y, MBG have alkaline affinity. Using the Nb*2-Zr/4-Y and Y/15-La/10-Nb/8 triangles and Zr/Y vs. Zr diagram, the MBG is within continental plate alkaline rock. The V vs. Ti diagram (Shervais, 1982) and Ti/500-Sm*50-V triangle (Vermeesch, 2006) indicate OIB alkaline affinity for MBG.

At the Moler and Groves (1993) discrimination diagrams such as, Zr/A_2O_3 vs. TiO_2/Al_2O_3 and

Ce/P_2O_5 vs. Zr/TiO_2, the MBG formed in the within plate and post-collisional fields (Fig. 6a-c). Also at the $(Nb/Zr)_N$ vs. Zr diagram (Thieblemont and Tegyey, 1994), MBG plot in the alkali, within plate rocks field (Fig. 6d).

Table 2) Trace elements concentrations of MBG.

	S72O	S78A	S79A	S74	S77	S73O	S80A	S85B
Ba	509	584	949	441	481	479	871	151
Co	36.2	45.5	45.6	48.4				
Cr	280	880	100	970	250	794	83	253
Cs	0.53	2.07	1.17	2.08				
Cu	217	147	96	73				
Ga	17.6	15.7	21.4	16	15	16	18	15
Hf	3.8	4	4.6	3.1				
Mo	22	2	3	2				
Nb	34.9	28.9	52.3	23.7	38	31	50	51
Ni	137	224	132	170	122	193	107	132
Pb	14	12	20	7				
Rb	25.3	20.8	37.6	15.2	16	8	22	26
Sn	2	1	2	1				
Sr	864	1095	1350	892	899	1116	1305	832
Ta	2.4	1.7	4.6	1.4				
Th	11.4	3.36	11.4	2.45				
U	3.38	0.78	2.11	0.57				
V	184	193	264	252	167	183	212	137
W	4	1	2	5				
Y	17.4	15.1	23.5	15.5	17	16	22	24
Zn	94	86	106	96	78	68	78	98
Zr	143	160	153	112	179	162	187	266

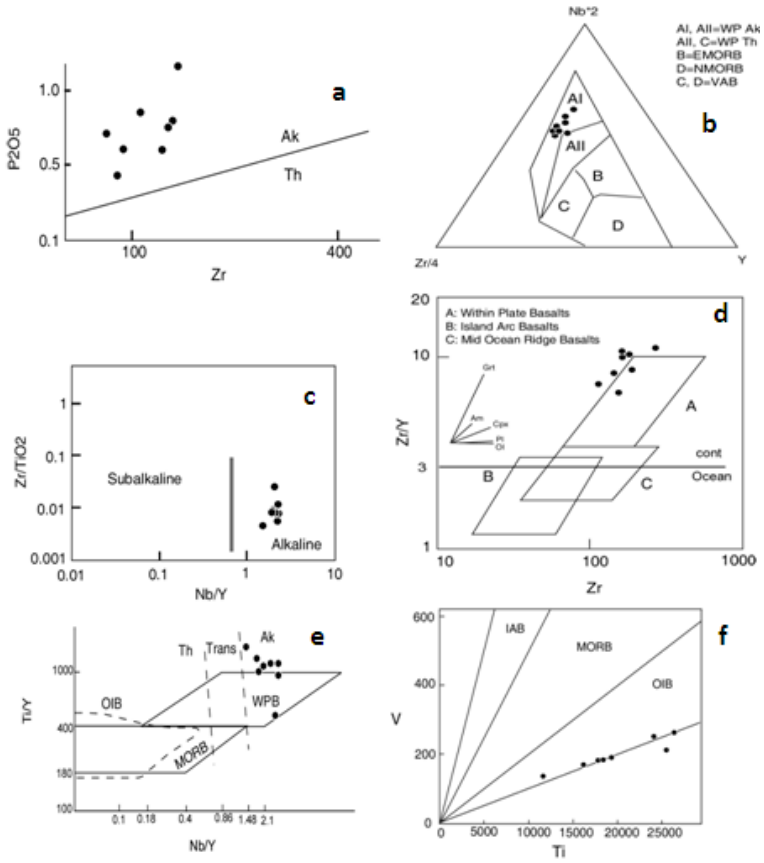

Figure 4) Various discriminations show that the MBG is alkaline within plate gabbro. a) Winchester and Floyd (1976), b) Meschede (1986), c) Vasquez and Althenberger (2005), d) Pearce (1983), e) Pearce (1982), f) Shervais (1982).

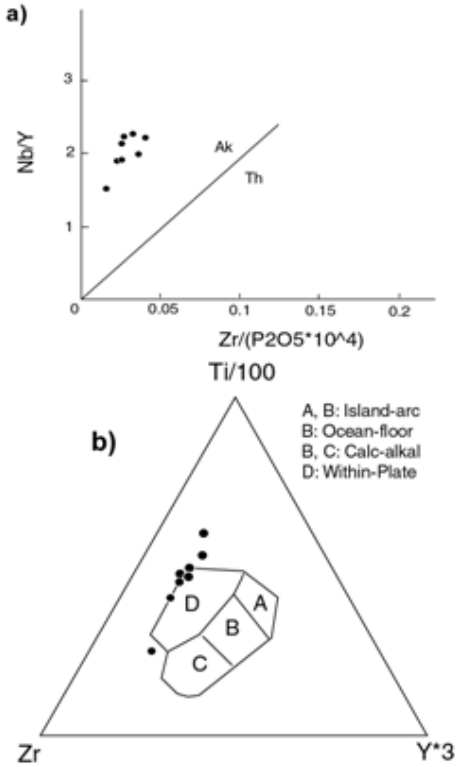

Figure 5) Diagrams determine the alkaline within plate setting for the MBGs. a, b) Floyd and Winchester (1975). c) Pearce and Cann (1973). d) diagram show that amphibole is the major mineral is crystallized from magma.

The steep REE pattern with enrichment of LREE respect for HREE (Fig. 3), indicates that garnet as a residual phase collect the HREE and were not contribute at the partial melting during magma generation. We use Sm/Yb vs. Sm and Sm/Yb vs. La/Sm ratios after Zhao and Zhou (2007) for confirmation the garnet-lherzolitic source and low degree of partial melting. Low degree of partial melting for alkaline gabbros, is supported by high concentration of LILEs (e.g. Dostal and Owen, 1998; Mertz *et al*., 2001; Weaver, 1991; Morata *et al*., 2005).

In order to determination the genesis of MBG, we compared the MBG REE pattern with various gabbros, which are formed at different tectonic settings (Fig. 7). The MBG REE pattern is very similar to Ngaoundere diorite from Cameroon (Tchameni *et al*., 2006), Pajaroto gabbro in the Andes-Colombia (Vasques and Altenberger, 2005) and mafic rocks at the Yamdrock mélange, Tibet (Dupuis *et al*., 2005) which are formed because of extension and rift generation at the ancient subduction settings. Enrichment of these gabbros has not any relationship with fluids derived from subducted oceanic crust.

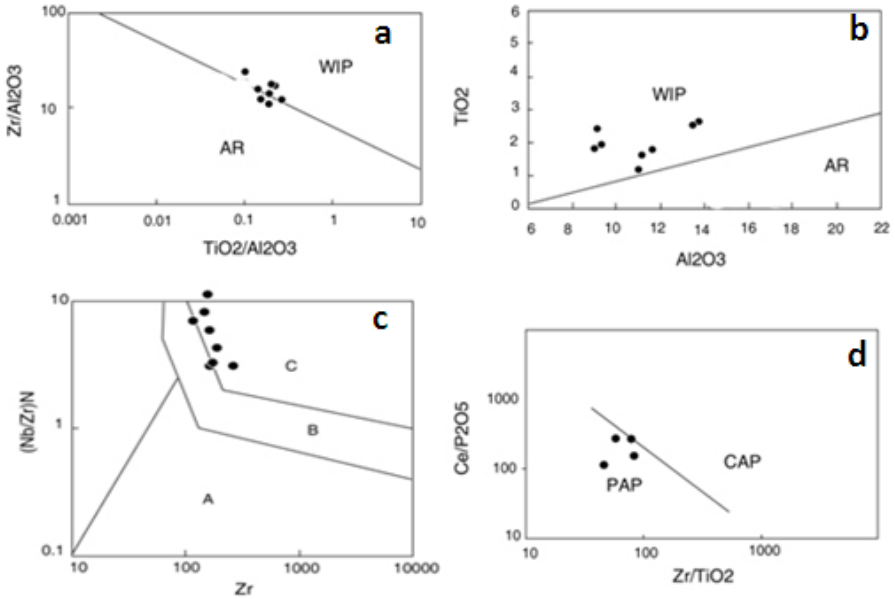

Figure 6 a-c) Discrimination diagrams (Muller and Groves, 1993) show that all of the MBGs are related to within plate. AR: arc related. WIP; within plate related, CAP; continental arc position, PAP; post collision position. d) Nb/Zr normalized to primitive mantle relation vs. Zr diagram (Thieblemont & Tegyey, 1994)

indicate intraplate setting for MBGs. A: subduction related magmatic rocks, B: continental collision setting, C: within plate alkaline rocks.

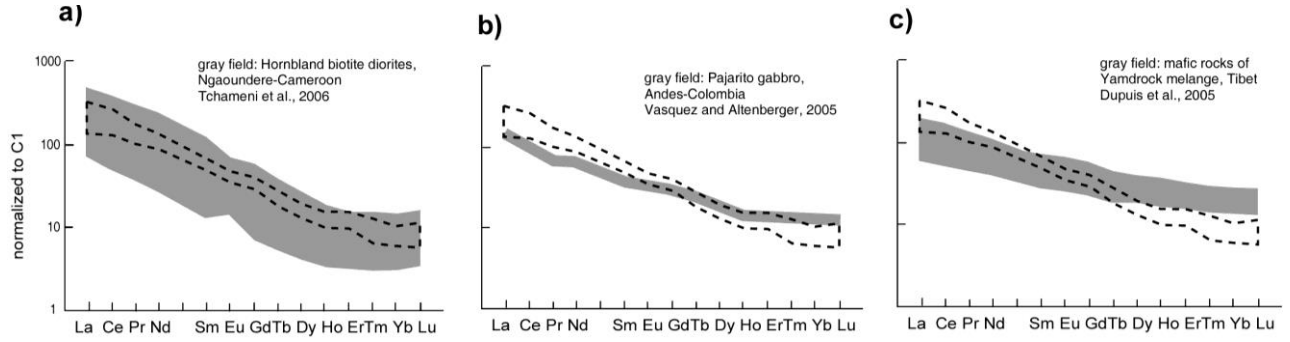

Figure 7) Comparison of MBG chondorite-normalized REE pattern, to three other gabbro. The dashed lines show range of composition for MBG.

Third case (Yamdrock, Tibet) is erupted at the OIB setting. There are very distinct differences between the MBG REE pattern and MORB or supra-subduction zone basalts REE patterns. The multi-elements diagrams of OIB, suggested by Sun and McDonough (1989) are identical with the MBG multi-elements diagram. There are miscorrelation between the MBG multi-elements diagram and EMORB (Sun and McDonough, 1989) and Izu arc basalts (Fig. 8), indicates that the MBG is not E-MORB or an arc related gabbro.

Table 3) Representative REE concentration of the MBG.

	S72O	S78A	S79AO	S74
La	53.4	43.2	70.2	33.4
Ce	108.5	96.2	150	81.5
Pr	11.95	11.45	16.55	10.75
Nd	45.4	47.4	62.4	46.1
Sm	7.62	7.99	10.2	8.4
Eu	2.03	2.11	2.76	2.25
Gd	6.17	6.15	8.44	6.49
Tb	0.75	0.71	1.03	0.76
Dy	3.67	3.43	4.92	3.57
Ho	0.66	0.58	0.9	0.62
Er	1.86	1.64	2.56	1.67
Tm	0.23	0.19	0.31	0.18
Yb	1.35	1.13	1.78	1.13
Lu	0.2	0.17	0.27	0.16
Y	17.4	15.1	23.5	15.5

7– Disscussion

The MBG samples primitive mantle normalized diagrams (normalization values from Sun and McDonough, 1989) show a significant Rb, Ba and K enrichment (Fig. 8) which indicates a primitive melt composition, as described by Mg, Ni and Cr contents. Zr and Ti have very gentle positive anomalies in the primitive mantle-normalized concentrations. Therefore, significant fractionation of specific Nb-, Zr-, and Ti-bearing phases during and after melt generation did not occur.

High primitive mantle-normalized ratios (such as: Sr_N/P_N (>2)) may indicate slab-derived fluids (Borg *et al*., 1997). Most samples of MBG have values lower than 1. Hence, MBGs are clearly without evidence of metasomatic fluids.

There are no negative anomalies for Ti, Ta and Nb in the MBG normalized to primitive mantle pattern (Fig. 8). High content of Nb and Ta is related to the within plate origin source for the MBG (Edwards *et al*., 1994; Zou *et al*., 2000). A very smooth positive peak for Th and U probably related to the source magma composition or low degree of partial melting. The Sm/Yb vs. Sm and Sm/Yb vs. La/Sm ratios (Aldanmaz, 2000) used for confirmation the garnet-lherzolitic source and low degree of partial melting. The primitive mantle-normalized multi-element diagram of the MBG shows a pattern of LILE and HFSE contents typical of OIB magmas generated in an intra-plate setting. The absence of a negative Nb anomaly argues against significant crystal contamination. The Yb_N values<10 (2.3-3.6) are

compatible with the presence of garnet as a residual phase in the mantle source. In order to determine the genesis of MBG, we compared the MBG multi-elements diagram with various gabbros, which are formed at different tectonic settings (Fig. 8). The trend is similar to OIB and Yamdrock, Tibet mafic rock patterns, but has obvious diverse with MORB and Arc basalts.

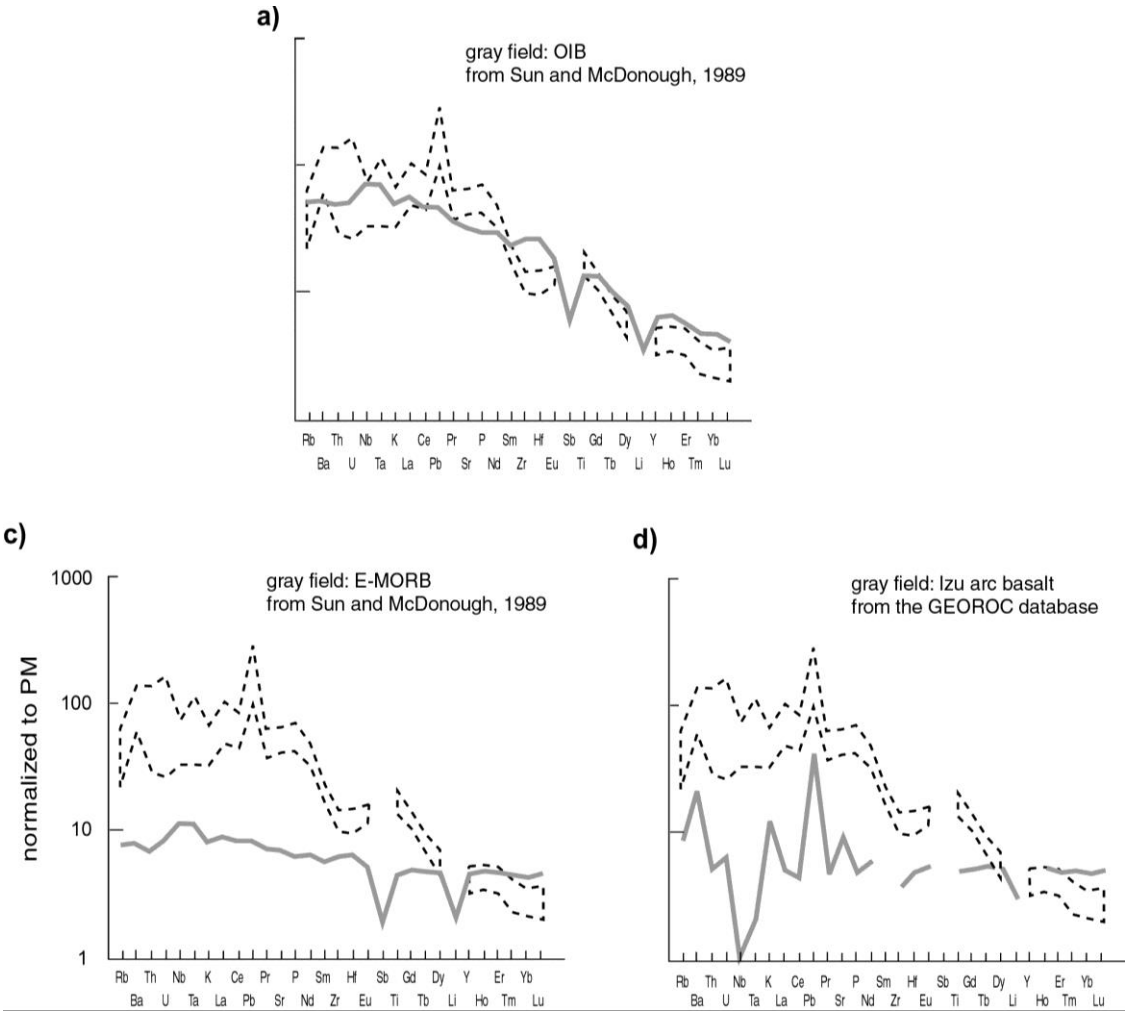

Figure 8) Multi-element to primitive mantle normalized pattern of MBG resembles to OIB pattern and Yamdrock mafic rocks.

Two distinct rock types were built during the Sanandaj-Sirjan magmatism generation: the diorite and granite suites (I-type granitic suits) were emplaced between 100 and 92Ma, whereas the younger suites (some A-type alkaline rocks) were emplaced between 82 and 80Ma (Ghalamghash *et al*., 2009).The first magmatic episode (100–92Ma) is regarded as subduction-related, whereas the second one (at ca 80Ma) likely occurred during the collision between the Arabian margin and the Sanandaj–Sirjan zone. Hence, it is possible that, the studied MBG is synchronous with the younger units of the Sanandaj-Sirjan stocks, introduced by Ghalamghash *et al*. (2009) or is younger than them, is formed during an extensional or transtensional tectonic position, when relaxation after collision is happened.

8– Conclusions

The MBG has high potassic calc-alkaline to shoshonitic affinity. The whole rock compositions are mostly Ti-and P-rich which is indicator of alkaline, within plate magmas. The highly incompatible elements concentrations (e.g. Nb: 23.7-52.3, La: 33.4-70.2) are similar to within plate gabbros. Additionally Zr/Y (6.5-10.6) and Zr/Nb (2.93-5.54) ratios further

support this assumption (Wood, 1980; Sun and McDonough, 1989; Willson, 1989). The observed high LaN/YbN ratio expose a low degree of partial melting at the source. The geochemical characteristics indicate that crustal material or oceanic crust derived fluids have not contribution at the MBG magma generation. High content of Nb and Ta is related to the within plate setting for the MBG. At the various discrimination diagrams the MBG display mostly non-orogenic affinity. The Sm/Yb vs. Sm and Sm/Yb vs. La/Sm ratios used for confirmation the garnet-lherzolitic source and low degree of partial melting. The MBG is formed during or after the collision between Arabian plate and SW part of Iran at Sanandaj-Sirjan belt location with alkaline, within plate, non-orogenic affinity.

Acknowledgments:

The authors would like to thank Dr. M. Jamshidi-Badr and Dr. S.A. Mazhari for their kind and careful comments that made the manuscript improved.

References:

Aghanabati, S.A. 2006. Geology of Iran, Geological Survey of Iran Publications, 586p.

Ahadnejad, V. 2013. Comparative review of the Northern Sanandaj-Sirjan Zone granitoids. Journal of Tethys: 2, 128–137.

Alavi, M. 2007. Structures of the zagros fold-thrust belt in Iran. American Journal of Science: 307:,1064–1095.

Aldanmaz, E., Pearce, J.A., Thirlwall, M.F., Mitchell, J. G. 2000. Petrogenetic evolution of late Cenozoic, post-collision volcanism in western Anatolia, Turkey Journal of Volcanology and Geothermal Research: 102, 67–95.

Berberian, M., King, C. P. 1981.Towards a paleogeography and tectonic evolution ofIran. Canadian Journal of Earth Sciences: 19, 210–265 .

Borg, L., E., Clynne, M. A., Bullen, T. D. 1997. The variable role of slab-derived fluids in the generation of a suite of primitive calc-alkaline lavas from the southernmost Cascades, California. Canadian Mineralogist: 35, 425–452.

Coulon, C., Megartsi, M., Fourcade, S., Maury, R. C., Bellon, H., Louni Hacini, A., Cotton, J.,Coutelle, A., Hermitte, D. 2002. Post collisional transition from calc-alkaline to alkaline volcanism during the Neogene in oranite (Algeria): magmatic expression of a slab breakoff. Lithos: 62, 87-110.

Darvish zadeh, A. 1990.Geology of Iran.Amirkabir Publications, 901p.

Dostal, J., Owen, J.V. 1998. Cretaceous alkaline lamprophyres from northeastern Czech Republic: Geochemistry and petrogenesis. Geologische Rundschdau: 87, 67–77.

Dupuis, C., Hebert, R., Dubois-Cote, V, Wang, C. S., Li, Y,L., Li, Z.J. 2005. Petrology and geochemistry of mafic rocks from melange and flysch units adjacent to the Yarlung Zangbo Suture Zone, Tibet. Chemical Geology: 214, 287–308.

Edwards, C. M. H., Menzies, M. A., Thirlwall, M. F., Morris, J. D., Leeman, W. P., Harmon, R. S. 1994. The transition to potassic alkaline volcanism in island arcs: the Ringgit-Beser complex, east Java, Indonesia. Journal of Petrology: 35, 1557–1595.

Ghalamghash, J., Nédélec, A., Bellon, H., Vousoughi Abedini, M., Bouchez J. L. 2009.The Urumieh plutonic complex (NW Iran): A record of the geodynamic evolution of the Sanandaj–Sirjan zone during Cretaceous times – Part I: Petrogenesis and K/Ar dating. Journal of Asian Earth Sciences 35, 401–415.

Griffiths, J.B., Gruau, G., Cornen, G., Azambre, B., Mage, J. 1997. Continental lithospheric contribution to alkaline magmatism: isotopic and geochemical evidence from Serra de Monchique and Mount Ormonde complexes. Journal of Petrology: 38, 115–132.

Haschke, M., Siebel, W., Gunther, A., Scheuber, E. 2002.Repeated crustal thickening and recycling during the Andean orogeny in north Chile. Journal of Geophysical Research: 107, ECV 6-1–ECV 6-18.

Hassanzadeh, J., Stockli, D.F., Horton, B.K., Axen, G.J., Stockli, L.D., Grove, M., Schmitt, A.K., Walker, J.D. 2008. U-Pb zircon geochronology of late Neoproterozoic–Early Cambrian granitoids

in Iran: implications for paleogeography, magmatism, and exhumation history of Iranian basement. Tectonophysics: 451, 71–96.

Hole, M.J., Saunders, A.D., Rogers, G., Sykes, M.A. 1995. The relationship between alkaline magmatism, lithospheric extension and slab window formation along continental destructive plate margins, in: Smellie, J.L. (Ed), Volcanism Associated with Extension at Consuming Plate Margins, Geological Society Special Publication: 81, 265–285.

Kholgi, M.H., Vosughi Abedini, M. 2004. Origin, petrogenesis and radiometric agedating of Pichaghchi batholite (North West Iran). Geosciences of Iran: 11 (No 49–50), 78–89.

Kholgi, M.H., Eghlimi, M.H., Amini Azar, R., Alavi Naini, M. 1994. Geological mapof Shahindezh 1:100000, Geological Survay of Iran Publications, 5363.

Mertz, D.F, Weinrich, A. J., Sarp, W.D., Renne, P.R., 2001. Alkaline intrusions in a near-trench setting, Franciscan complex. California: constraints from geochemistry, petrology, and Ar chronology. American Journal of Sciences: 301, 877–911.

Middlemost, E.A.K. 1991.Towards a comprehensive classification of igneous rocks and magmas. Earth Sciences Review: 31, 73–87.

Modjarrad, M. 2007a. Petrology and geodynamics of metamorphic and igneous rocks of Shahindezh-NW Iran, Unpublished PhD thesis, University of Tabriz, Tabriz-Iran, 190p.

Modjarrad, M., Moazzen, M., Moyyed, M. 2007b. Contact metamorphism in theShahindezh Metamorphic Core (SMC)-NW Iran; PT conditions and microstructural evidence for partial melting of metapelites. Iranian Journal of CrystallographyMineralogy: 15, 493–514.

Modjarrad, M., Moazzen, M., Moayyed, M. 2008.HT-MP metamorphism at theShahindezh Metamorphic Core (SMC)-NW Iran; Mineral chemistry and thermobarometry of metapelites.Iranian Journal of Crystallography and Mineralogy: 16, 3–12.

Modjarrad, M., Moazzen, M., Moayyed, M. 2010. Whole rock chemistry of Shahindezh metapelites, provenance and mineral parageneses. Petrology (Isfahan Uni.): 4, 73–88.

Mohajjel, M., Fergusson, B.C.L., Sahandi, M.R. 2003.Cretaceous–Tertiary convergence and continental collision, Sanandaj–Sirjan Zone, western Iran. Journal of Asian Earth Sciences: 21, 397–412.

Muller, D., Groves, D.I. 1993.Direct and indirect associations between potassic igneous rocks, shoshonites and gold-copper deposites. Ore Geology Review: 8, 383–406.

Morata, D., Claudia, O., Cruz, R., Manuel, S. 2005. The Bandurrias gabbro: Late Oligocene alkaline magmatism in the Patagonian Cordillera. Journal of South American Earth Sciences: 18, 147–162.

Nakamura, E., Campbell, I. H., McCulloch, M. T., Sun, S. S. 1989. Geochemical Geodynamics in a back arc region around the Sea of Japan: implications for the genesis of alkaline basalts in Japan, Korea and China. Journal of Geophysical Research: 94, 4634–4654.

Ngounouno, I., Moreau, C., Deruelle, B., Demaiffe, D., Montigny, R. 2001. Petrologie du complex alcalin sous-sature de Kokoumi. Bulletin de la Societe geologique de la France 172: 675–686.

Ramos, V. A., Kay, S. M. 1992. Southern Patagonian plateau basalts and deformation: back arc testimony of ridge collisions. In: Oliver, R. A., (eds), Andean Geodynamics Tectonophysics: 205, 261–282.

Rickwood, P.C. 1989. Boundary lines within petrologic diagrams which use oxides of major and minor elements. Lithos: 22, 247–363.

Shervais, J. W. 1982. Ti-V plots and petrogenesis of modern and ophiolitic lavas. Earth and Planetary Sciences Letters: 23, 319–351.

Shinjo, R., Woodhead, J. D., Hergt, J. M. 2000. Geochemical variation within the northern Ryukyu Arc: magma source compositions and geodynamic implications. Contributions to Mineralogy and Petrology: 140, 263–282.

Stern, C.R., Frey, F.A., Kiyoto, F., Zartman, R.E., Peng, Z., Kyser, T.K. 1990. Trace element and Sr, Nd, Pb, and O isotopic composition of Pliocene and Quaternary alkali basalts of the Patagonian Plateau lavas

of southernmost South America. Contributions to Mineralogy and Petrology: 104, 294–308.

Stern, C. R., Kilian, R. 1996. Role of the subducted slab, mantle wedge and continental crust in the generation of adakites from the Andean Austral Volcanic Zone. Contributions to Mineralogy and Petrology: 123, 263–281.

Sun, S.S., McDonough, W.F. 1989. Chemical and isotopic systematic of oceanic basalts: implications for mantle composition and processes. In: Saunders, A.D. Norry, M.J.(eds), Magmatism in the Ocean Basins. Geological Society, London, Special Publications: l42, 313–345.

Tchameni, R., pouclet, A., Penaye, J., Ganwa, A.A., Toteu, S.F. 2006. Petrography and geochemistry of the Ngaoundere pan-African granitoids in Central North Cameroon:Implications for their sources and geological setting. Journalof African Earth Sciences: 44, 511–529.

Thieblemont, D., Tegyey, M. 1994. Une discrimination geochimique des rochesdifferenciees temoni de la diversited origine et de situation tectonique des magmascalco-alcalins. Comptes Rendus Academic Sciences: 319, 87–94.

Vasques, M., Altenberger, U. 2005.Mid-Cretaceous extension-related magmatism in the eastern Colombian Andes. Journal of South American Earth Sciences: 20, 193–210.

Vermeesch, P. 2006. Tectonic discrimination of basalts with classification trees. Geochimica et Cosmochimica Acta: 70, 1839–1848.

Weaver, B.L. 1991. Trace element evidence for the origin of ocean-island basalts. Geology: 19, 123–126.

Woodhead, J. D., Eggins, S., Gamble, J. 1993. High field strength and transition element systematics in island arc and back-arc basin basalts: evidence for a multiphase melts extraction and a depleted mantle wedge. Earth and planetary Sciences Letters: 144, 491–504.

Willson, M. 1989. Igneous Petrogenesis. Boston Sydney Wellington, Unwin Hyman, London.

Wilson, M., Downes, H. 1991.Tertiary-Quaternary extension-related alkaline magmatism in Western and Central Europe. Journal of Petrology: 32, 811–849.

Wilson, M., Downes, H., Cebria, J.M. 1995.Contrasting fractionation trends in coexisting continental alkaline magma series; France.Journal of Petrology: 36, 1729–1735.

Wood, D. A. 1980. The application of a Th-Hf-Ta diagram to problems of tectonomagmatic classi_cation and to establishing the nature of crustal contamination of basaltic lavas of the British Tertiary volcanic province. Earth and Planetary Sciences Letters: 50, 11–30.

Zhao, J.H., Zhou, M.F. 2007. Geochemistry of Neoproterozoic mafic intrusions in the Panzhihua district (Sichuan Province, SW China): Implications for subduction-related metasomatism in the upper mantle. Precambrian Research: 152, 27–47.

Zou, H. B., Zindler, A., Xu, X. S., Qu, Q. 2000. Major. Trace elements and Nd, Sr and Pb isotope studies of Cenozoic basalts in SE China: mantle source, regional variations, and tectonic significance. Chemcal Geology: 171, 33–47.